



Identification of calretinin-expressing retinal ganglion cells projecting to the mouse superior colliculus

Eun-Shil Lee¹ · Jea-Young Lee² · Gil Hyun Kim¹ · Chang-Jin Jeon¹

Received: 2 May 2018 / Accepted: 12 November 2018 / Published online: 3 December 2018
© Springer-Verlag GmbH Germany, part of Springer Nature 2018

Abstract

In mice, retinal ganglion cells (RGCs), which consist of around 30 subtypes, exclusively transmit retinal information to the relevant brain systems through parallel visual pathways. The superior colliculus (SC) receives the vast majority of this information from several RGC subtypes. The objective of the current study is to identify the types of calretinin (CR)-expressing RGCs that project to the SC in mice. To label RGCs, we performed CR immunoreactivity in the mouse retina after injections of fluorescent dye, dextran into mouse SC. Subsequently, the neurons double-labeled for dextran and CR were iontophoretically injected with the lipophilic dye, DiI, to characterize the detailed morphological properties of these cells. The analysis of various morphological parameters, including dendritic arborization, dendritic field size and stratification, indicated that, of the ten different types of CR-expressing RGCs in the retina, the double-labeled cells consisted of at least eight types of RGCs that projected to the SC. These cells tended to have small-medium field sizes. However, except for dendritic field size, the cells did not exhibit consistent characteristics for the other morphometric parameters examined. The combination of a tracer and single-cell injections after immunohistochemistry for a particular molecule provided valuable data that confirmed the presence of distinct subtypes of RGCs within multiple-labeled RGCs that projected to specific brain regions.

Keywords Calretinin · Retinal ganglion cells · Retrograde tracer injection · Single-cell injection · Superior colliculus

Introduction

Retinal ganglion cells (RGCs) are the primary projection neurons of the retina and they generate nerve impulses to transmit visual and non-visual information to various brain areas through their axons. RGCs consist of distinct subclasses of cells that are selectively stimulated by specific types of information that they transmit to different brain areas, such as the thalamus, hypothalamus and midbrain, through parallel pathways (Berson 2008; Dhande and Huberman 2014; Sanes and

Masland 2015). For example, M-type RGCs project to the magnocellular layers of the lateral geniculate nucleus (LGN), P-type RGCs project to the parvocellular layers of the LGN and non-M, non-P RGCs project to the koniocellular layers of the LGN (Callaway 2005; Schmolesky 1995-2005). In addition, intrinsically photosensitive RGCs (ipRGCs), which contain the photopigment melanopsin, consist of five subtypes characterized by their distinctive morphologies. Among the ipRGC subtypes, the Brn3b-negative M1 type mainly projects to the suprachiasmatic nuclei (SCN) of the hypothalamus and the Brn3b-positive M1 type mainly projects to the olivary pretectal nucleus in the midbrain (Hattar et al. 2002). These different subtypes are sensitive to the circadian clock and pupillary light reflexes, respectively (Chen et al. 2011). In addition, the postsynaptic targets of the M4 RGCs are the LGN and superior colliculus (SC), the functions of which are not yet clear (Dhande and Huberman 2014; Ecker et al. 2010). Thus, these findings indicate that diverse subtypes of RGCs have distinct projection targets and functions.

In order to determine where distinct RGC subtypes project in the brain, these RGCs need to be classified. At least four

Eun-Shil Lee and Jea-Young Lee contributed equally to this work.

✉ Chang-Jin Jeon
cjjeon@knu.ac.kr

¹ Department of Biology, School of Life Sciences, BK 21 Plus KNU Creative BioResearch Group, College of Natural Sciences, and Brain Science and Engineering Institute, Kyungpook National University, Daegu 41566, South Korea

² Center of Excellence for Aging and Brain Repair, USF Health, University of South Florida, Tampa, FL 33612, USA

criteria are used to classify RGCs (Roska and Meister 2014; Sanes and Masland 2015). First, mice RGCs have been classified based on their uniform morphological characteristics, such as dendritic branching pattern, dendritic stratification of the inner plexiform layer (IPL), soma size and dendritic field size, using various methods. For example, 14 distinct subtypes of RGCs been morphologically characterized using DiI particle bombardment (Sun et al. 2002). Badea and Nathans (2004) have described at least 12 RGC types using a genetically directed reporter. Kong et al. (2005) and Coombs et al. (2006) classified 11–14 RGC types in mice using cellular labeling methods. Völgyi's group classified RGCs into at least 22 types using Neurobiotin injections (Völgyi et al. 2009). Second, RGCs are also characterized using molecular markers. For example, the junctional adhesion molecule-B (JAM-B) has been used in mice to identify a subset of OFF RGCs that exhibit direction selectivity (Kim et al. 2008). The W3 type in the TYW3 mouse transgenic line, which has specific feature detectors, is equivalent to the B2 type classified by Sun's group (Zhang et al. 2012). In addition, the cocaine- and amphetamine-regulated transcript (CART) is a selective neuropeptide marker of all ON-OFF direction-selective RGCs (DSGCs) (Kay et al. 2011). Third, at least 12 functional types of mice RGCs have been distinguished based on physiological features using spike output recordings (Farrow and Masland 2011). At least 30 functional types of RGCs were recently characterized by their light responses and morphology using two-photon calcium imaging (Baden et al. 2016). Fourth, single cells in the retina have been traced and characterized using their spatial mosaic arrangement (Rockhill et al. 2000).

The SC, which is part of the tectum in the midbrain, is the second most notable retinal recipient area after the LGN. It receives direct input from about 85–90% of RGCs in the mice (Ellis et al. 2016). The SC is a multilayered structure with its cell bodies and fibers located in two main layers: the superficial and deeper layers. The SC contains a topological map because layer subsets receive outputs from axons serving other areas. The neurons in the superficial layers, which respond to visual stimuli, synapse with axons arising from RGCs or projection neurons in the primary visual cortex. In particular, of the RGC subtypes, inputs from ON-OFF direction-selective (Huberman et al. 2009; Kay et al. 2011; Rivlin-Etzion et al. 2011), W3, J and alpha RGCs have been shown to project to the superficial layers of the SC (Hofbauer and Dräger 1985; Huberman et al. 2008; Kim et al. 2010). However, neurons in the deeper layers, which respond to multimodal sensory stimuli, synapse with projection neurons in the extrastriate cortex, other somatosensory-related cortical areas and RGCs, such as ipRGCs (Cang and Feldheim 2013; Hattar et al. 2006; Huberman et al. 2008; Jonathan and Hiroshi 2017; May 2006). Thus, the neuroanatomical structure of the SC is well suited for the association of the visual sensory and motor systems and its functions include sensorimotor integration,

such as inducing eye and head movement according to spatial information from the retina (Stein et al. 2002).

Calcium is a key molecule in most essential cellular processes. Calretinin (CR), which is a calcium-binding protein, has been used to characterize specific cell populations in the brain as well as the retina. In the mouse retina, the CR antibody labels specific cell types, amacrine cells, bipolar cells and cell bodies in the ganglion cell layer (GCL) (Haverkamp and Wässle 2000; Lee et al. 2010). Moreover, we confirmed in our quantification study that CR is located in a subset of RGCs. As previously mentioned, the ipRGC subtypes, M1 cells, are further subdivided into two types according to their expression of the Brn3b transcription factor. These two subtypes have the same morphological and electrophysiological properties but project to different brain targets: the SCN or olivary pretectal nucleus (Hattar et al. 2002; Chen et al. 2011). Therefore, even if cells have the same morphological characteristics, their major brain targets might differ in accordance with the expression of specific molecules and their functional properties might differ.

RGC subsets that express particular proteins innervate distinct retinal recipient areas of the brain through parallel pathways and might serve different visual functions. Our study aims to investigate multiple SC-projecting RGC subtypes with distinctive morphologies that contain CR detected by using a triple-labeling technique involving retrograde tracer injections and single-cell injections of lipophilic dye following immunohistochemistry.

Materials and methods

Animals and retrograde tracer injection

The experiments were performed on adult C57/BL6 mice of both sexes ($n = 38$). The mice were deeply anesthetized using intramuscular injections of a ketamine hydrochloride (30–40 mg/kg) and xylazine (3–6 mg/kg) mixture and then mounted in a stereotaxic apparatus. A small craniotomy was then made above the SC and a 5- μ L Hamilton microsyringe filled with dextran solution (1–3 μ L of a 5% solution of tetramethylrhodamine [3000 MW] in phosphate buffer [PB, pH 7.4; Thermo Fisher Scientific Inc., Waltham, MA, USA]) was fitted to the stereotaxic system. Because of a retinotopic map into the SC (Ito and Feldheim 2018), all dextran injections were made in various SC areas along the anterior-posterior axis and lateral-medial axis that were identified by the stereotaxic coordinates in a mouse brain atlas (between –4.0 and –4.4 mm posterior to the bregma, 0.6–1.4 mm lateral to the midline and 1.0–1.5 mm ventral to the dural surface, Hof et al. 2000). The animals were placed alone in clean cages and allowed to recover. After a 48 h recovery, the animals were perfused. The use of the animals was performed

according to the National Institutes of Health guidelines for the use and care of animals. The study was also approved (permission NO. 2015-0104) by the animal rights committee at Kyungpook National University, Daegu, South Korea.

Perfusion and tissue processing

The animals were anesthetized with the same mixture described above. Immediately, after eye enucleation, the retinas were carefully isolated from the eyecup and adhered ganglion-cell-side up to black non-fluorescent filter membranes (MilliporeSigma, Burlington, MA, USA). The filter membrane and attached retina were fixed for 30 min in 4% paraformaldehyde in 0.1 M PB (pH 7.4). The mice were perfused through the left ventricle-aorta with rinse and fixation solutions. Following a pre-rinse with the rinse solution containing approximately 30 mL of phosphate-buffered saline (PBS, pH 7.4) for 3–5 min, each mouse was fixed with 30–50 mL of paraformaldehyde containing 0.3–0.5% glutaraldehyde and 0.002% calcium chloride buffered for 20–30 min. Their heads were then removed and placed in the fixation solution for 2–3 h. The brains were then removed from the skulls, postfixed for 2–3 h in the same fixative and then stored overnight in 0.1 M PBS (pH 7.4) containing 8% sucrose and 0.002% calcium chloride. The SC was extracted, mounted onto a chuck and cut into 50- μ m-thick sections with a Vibratome. The sectioned tissues were covered with coverslips and Vectashield mounting medium (Vector Laboratories, Inc., Burlingame, CA, USA).

Fluorescent immunohistochemistry

For single-cell injection, after rinses of retinas, we used immunohistochemical techniques without using detergents (Kim and Jeon 2006). Briefly, a primary antibody against CR (Thermo Fisher Scientific Inc.) was applied at a 1:100–200 dilution in 0.1 M PB for 2 h. After incubation and washes in 0.1 M PB, the retinas were incubated with the FITC-conjugated goat anti-rabbit IgG secondary antibody (1:50; Vector Laboratories, Inc.) in 0.1 M PB for 1–2 h and then we performed single-cell injection for classification of cells.

For dual immunostaining for CR and parvalbumin (PV), we performed by following a conventional technique (Jeon et al. 1998). The primary antibodies and concentrations used were mouse anti-CR antibody (1:500, Thermo Fisher Scientific Inc.) and rabbit anti-PV antibody (1:500, Swant, Bellinzona, Switzerland). The secondary antibody used for immunofluorescence detection was as follows: FITC-conjugated anti-mouse IgG (1: 250; Vector Laboratories, Inc.) and cyanine 3 (Cy3)-conjugated anti-rabbit IgG (1: 250; Jackson ImmunoResearch Laboratories, Inc., West Grove, PA, USA). The tissues were coverslipped using Vectashield mounting medium (Vector Laboratories, Inc.).

Immunofluorescence images were obtained using a Bio-Rad MRC 1024 confocal microscope (Bio-Rad Laboratories, Inc., Hercules, CA, USA).

Single-cell injections

The methods used for the single-cell injections following the immunohistochemistry on whole-mount retina were similar to those we previously used for mouse and rabbit ganglion cell injections (Kao and Sterling 2003; Kim and Jeon 2006; Kwon et al. 2014; Lee et al. 2010). In brief, the FITC- and dextran-labeled cells were viewed with a microscope equipped with a Zeiss 40X Plan Achromat (NA, 0.80) water-immersion lens and Zeiss filter set 09 (excitation, 450–490 nm; emission, 515 nm). The tips of the electrodes were filled with the 1% lipophilic dye, DiI (Thermo Fisher Scientific Inc.), in ethanol. The colocalized cells were filled iontophoretically by passing a positive current of 5–20 nA and 0.2–0.5 mV with 1% DiI. The optimal filling time was 15–30 min. However, dextran-filled CR-expressing retinotectal cells were injected only in the midperiphery of the retina, 1.0–1.7 mm away to the optic disc, because dendritic field size may vary according to retinal eccentricity. Once a selected cell was filled, an indexed grid reticle was moved laterally and another cell in the near-center of the grid was injected. After several cells in the retina were filled, the retina was placed in 4% paraformaldehyde in 0.1 M PB for 2 h. To counterstain the tissue, the retina was immersed for 1 h in the nucleic acid-staining dye SYTO13 (Thermo Fisher Scientific Inc.). The tissue was then rinsed in 0.1 M PB and coverslipped with Vectashield mounting medium (Vector Laboratories, Inc.).

Data analysis

The cells were scanned with a Bio-Rad MRC 1024 confocal microscope equipped with a 40X objective (NA 0.75; Plan Fluor; Nikon Corporation, Tokyo, Japan). Two sets of z stacks were collected for each injected cell. First, we scanned the DiI-filled cell from the soma in the GCL to the last of the dendrites at 1- μ m intervals by z-series reading on the confocal microscope using an emission filter (580DF32; Chroma Technology Corporation, Bellows Falls, VT, USA). Subsequently, the through-focus method was used to image the nucleic acid-stained nuclei (SYTO13; Thermo Fisher Scientific Inc.) and images were collected at 1- μ m intervals using an emission filter (515DF30; Chroma Technology Corporation) in order to measure the thickness of the IPL and determine the level at which the dendritic processes of the DiI-filled cells stratified in the IPL. The depth of the GCL/IPL boundary was defined as 100, while the depth of the IPL/inner nuclear layer boundary was defined as 0. The z coordinate of each dendritic branch was defined as the distance between the GCL/IPL and IPL/inner nuclear layer boundaries. The number of

primary dendrites that emerged from the soma was counted in the confocal z-series images and the dendritic field areas and diameters were measured (AxioVision 4; Carl Zeiss Meditec, Inc., Dublin, CA, USA) by connecting the distal-most tips of the dendrites (Rodieck 1998). These data were used to illustrate the branching and level of stratification of each type of neuron in Adobe Photoshop (Photoshop CS6; Adobe Systems, Inc., Mountain View, CA, USA). Somal size could not be assessed in this study because of the strong fluorescent halo on the cell body. All data are presented as mean \pm standard deviation.

Quantitative analysis

For quantification, all experiments were performed on three retinas. CR-expressing retinotectal cells were expressed as the percentage of retinotectal cells that colocalized with CR. In the fluorescence-reacted whole mount retina, CR-expressing retinotectal cells were viewed on the computer monitor using a Zeiss Plan-Apochromat 40x objective (Carl Zeiss Meditec, Inc., Dublin, CA, USA) and an AxioCam HRc digital camera. Retinotectal cells were counted within four areas ($300\ \mu\text{m} \times 300\ \mu\text{m}$) per retina. Percentages of CR-expressing retinotectal cells per area were used to calculate average colocalization with a standard error of the mean (SEM). In this manner, quantitative analyses of CR and PV colocalization were also performed in the three mouse retinas.

Brain clearing

To confirm the injection site of SC, injected brains with dextran were cleared using the Binaree Brain Clearing kit (Cat. SHBC-001, Binaree, Korea). Briefly, fixed brains were immersed in fixing solution for 24 h and incubated with tissue clearing solution in a shaking incubator at 35 °C for 18 h and rinsed in washing solution. The brains were incubated in mounting and storage solution for 24 h (Cat. SHMS-050, Binaree, Korea) for further clearing. Light-sheet imaging of cleared samples was performed using mounting and storage solution (Cat. SHMS-050, Binaree, Korea) as the mounting medium.

Light-sheet microscopy

The cleared brain following dextran injection into SC was imaged using a Lightsheet Z.1 fluorescence microscope (Carl Zeiss Meditec, Inc.) with a $5\times/0.1$ dual side illumination optic and Plan-neofluar $5\times/0.16$ objective lens (Carl Zeiss Meditec, Inc.). Fluorescence was excited with 561 nm lasers and emission was detected with 575–615 nm band-pass filters. All image data of LSFM were saved as czi file type of ZEN software (Carl Zeiss Meditec, Inc.) and images were reconstructed and 3D rendered using Arivis vision 4D software

(arivis-AG, Rostock, Germany) and Imaris software (Bitplane, USA). Whole LSFM images and image rendering data were acquired in the Brain Research Core Facility (BRCF) at the Korea Brain Research Institute.

Results

Retrograde tracer injections into the SC

Retrograde tracer injections into the SC can be used to retrogradely trace axons extending from the RGCs, which are called retinotectal cells. To identify SC-projecting RGCs, we injected the fluorescent tracer dextran into superficial layers of the SC but some tracer diffused into the other layers of the SC (Fig. 1a). The contralateral RGC projecting to the superficial layer of the SC is configured to project the temporal-nasal axis of the retina along the anterior and posterior axis of the SC and the dorsal-ventral axis is projected along the lateral-medial axis of the SC. Dextran-filled RGCs were observed topographically aligned with the injection site of SC (Fig. 1b, c).

To confirm that CR-expressing RGCs projected to the SC, we performed immunohistochemistry with a CR antibody in the retrogradely labeled retina. Retrogradely labeled RGCs (Fig. 2a) and CR-positive cells were found (Fig. 2b) and some cells were double-labeled with the fluorescent tracers and CR (arrows in Fig. 2c). Therefore, the cells indicated by the arrows in Fig. 2(c) were CR-expressing retinotectal cells. In the quantitative analysis of retinotectal cells and CR colocalization, only few retinotectal cells were CR-positive ($18 \pm 4\%$). Single-cell injections of the lipophilic fluorescent compound DiI were applied to these cells to identify their morphological features.

The morphological features of the CR-expressing retinotectal RGCs

In the present study, 119 triple-labeled RGCs were analyzed using a laser scanning confocal microscope. The CR-expressing retinotectal cells were classified by various morphological parameters (dendritic branching pattern, dendritic morphology, dendritic field size and level of stratification within the IPL). The analysis of these characteristics resulted in at least eight types of CR-expressing RGCs. We gave these CR cell types the simple names of CR1 through CR8 (CR1–8; Table 1). Each cell type corresponded to mouse RGC subtypes described in previous studies by morphological criteria and transgenic markers. In addition, we used the exemplary descriptions of the morphologies of the functional types of RGCs in Baden et al. (2016) to try to match the functional types with the morphologies of the CR-expressing retinotectal

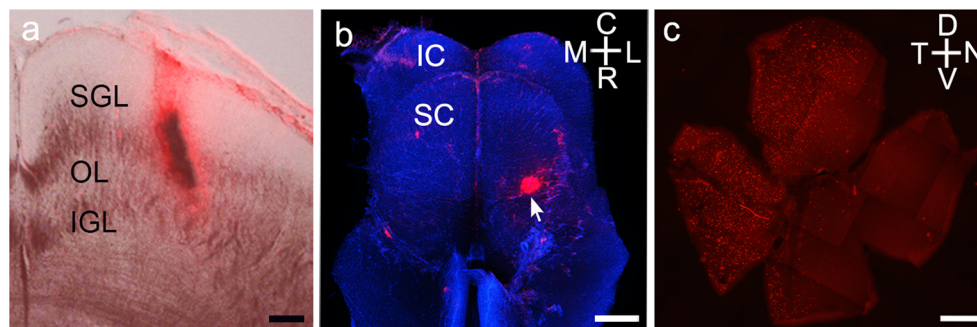


Fig. 1 Retrograde fluorescent dextran injection into the mouse superior colliculus. **(a)** Photomicrograph of the coronal section of the superficial layers of the superior colliculus that was injected with the fluorescent tracer dextran. **(b)** Light-sheet microscope imaging of the dorsal view of cleared superior colliculus where the fluorescent tracer dextran was injected (cleared brain counterstained with DAPI). Arrow is injection site

into superior colliculus, and **(c)** distribution of retrogradely labeled ganglion cells after injections into the superior colliculus. IC, inferior colliculus; IGL, intermediate gray layer; OL, optic layer; SC, superior colliculus; SGL, superficial gray layer; C, caudal; D, dorsal; L, lateral; M, medial; N, nasal; R, rostral; T, temporal; V, ventral. Scale bars = 100 μm **(a)** or 700 μm **(b)** or 500 μm **(c)**

RGCs. The descriptions of the cells are arranged in order of their dendritic field diameters.

The CR1 cells had medium-dense branches and some bi-directional branches overgrew the basal dendrites at regular intervals. Tiny branches, such as spines, were sometimes observed along the dendrites (Fig. 3a, a'). The CR1 cells had small dendritic fields and their dendrites ramified in the outer part of the IPL (Table 1 and Fig. 3a''). The morphological features of the CR1 cells were equivalent to the B4 RGCs (Sun et al. 2002), monostriated cluster 2 and 4 cells (Badea and Nathans 2004), cluster 1 cells (Kong et al. 2005), M11 cells (Coombs et al. 2006) and G8 cells (Völgyi et al. 2009) noted in previous studies of the mouse retina.

The CR2 cells had small dendritic fields and their short dendrites extended in a tortuous manner at many branch points and dendrites sometimes overlapped. The CR2 and CR1 cells looked similar but the CR2 cells had denser and more compact branches (Fig. 3b, b'). Their dendrites ramified in the outer part of the IPL (Table 1 and Fig. 3b''). The CR2 cells clearly corresponded to type B2 (Sun et al. 2002), monostriated cluster 4 cells (Badea and Nathans 2004), cluster 1 cells (Kong et al. 2005), M11 cells (Coombs et al. 2006), G5 cells (Völgyi et al. 2009) and W3 cells (Zhang et al. 2012) in the mouse retina.

The CR3 cells had a medium dendritic field. The CR3 cells had tiny sparse dendrites that produced many long and moderately wavy branches before ending at the dendrite terminals. Their dendritic arbors tended to be asymmetric (Fig. 3c, c'). The CR3 cells ramified in the outer part of the IPL (functionally described as the OFF variety) or the inner part of the IPL (functionally described as the ON variety, Table 1 and Fig. 3c''). The morphological features of the inner CR3 cells were similar to the inner B3 type (Sun et al. 2002), monostriated cluster 9 cells (Badea and Nathans 2004), cluster 4 cells (Kong et al. 2005), M7 (on) and M3 (on) cells (Coombs et al. 2006), and G6 cells (Völgyi et al. 2009) noted previously in the mouse retina. The morphological features of the outer CR3 cells were similar to the outer B3 type (Sun et al. 2002), monostriated cluster 1 cells (Badea and Nathans 2004), cluster 2 cells (Kong et al. 2005), cluster M3 (off) cells (Coombs et al. 2006) and the G7 type (Völgyi et al. 2009) in the mouse retina.

The CR4 cells had medium dendritic fields and their primary dendrites emerged from the cell body and then immediately and repetitively branched into secondary dendrites. Because these dendrites divided often into many long and relatively straight branches at regular intervals, several interdendritic spaces were observed between neighboring

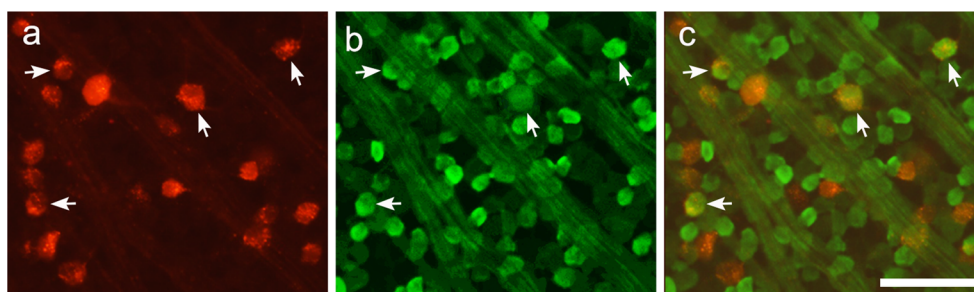


Fig. 2 Calretinin-expressing retinotectal cells labeled with the retrograde fluorescent tracer, dextran, in whole-mounted mouse retina 48 h after application of the dye to the superior colliculus. **(a)** Retinotectal cells and **(b)** calretinin immunoreactivity in the ganglion cell layer of the retina

at the same region. **(c)** Merged image of retinotectal cells and calretinin. Arrows indicate calretinin-expressing retinotectal cells. Scale bar = 50 μm

Table 1 Quantitative data of calretinin-positive mouse retinotectal RGC

Cell type	Dendritic field position (% of IPL depth) mean ± SD	Number in sample	% of total ganglion cell filled	Dendritic field diameter (µm) mean ± SD	Dendritic field area (µm ²)
CR1	41.55 ± 14.62	10	8.41	141 ± 20	10,650
CR2	38.28 ± 13.14	33	27.74	145 ± 28	12,449
CR3 ^a	56.85 ± 7.70 28.12 ± 7.76	8 7	12.60	205 ± 37 239 ± 25	19,877
CR4	47.97 ± 11.49	15	12.60	198 ± 21	19,535
CR5	50.47 ± 17.80	16	13.44	203 ± 35	23,149
CR6	43.67 ± 12.54	15	12.60	208 ± 36	23,195
CR7 ^b	71.52 ± 5.91 25.16 ± 8.11	6	5.04	226 ± 36	26,629
CR8 ^a	61.64 ± 9.59 33.08 ± 8.21	7 2	7.57	222 ± 43 281 ± 21	31,027
Total		119	100		

^a Monostratified cell type with ON and OFF populations

^b Bistratified cell type

dendritic branches (Fig. 4a, a'). Their dendrites ramified in layer 3 of the IPL (Table 1 and Fig. 4a''). CR4 cells obviously corresponded to type C4 (Sun et al. 2002), monostratified clusters 4 and 5 cells (Badea and Nathans 2004), cluster 1 cells (Kong et al. 2005), cluster M11 cells (Coombs et al. 2006) and G13 cells (Völgyi et al. 2009) in the mouse retina.

The CR5 cells had medium dendritic fields. Typically, CR5 cells had 5–7 primary dendrites with long and curvy and sometimes short branches at irregular intervals. Some branches stretched out infrequently and perpendicularly from the primary dendrites and few dendritic processes crossed each other (Fig. 4b, b'). Their dendrites ramified in layer 3 of the IPL (Table 1 and Fig. 4b''). The CR5 cells were equivalent to the B1 RGCs (Sun et al. 2002), monostratified cluster 1 cells (Badea and Nathans 2004), cluster 2 cells (Kong et al. 2005), M3 (off) cells (Coombs et al. 2006) and G4 cells (Völgyi et al. 2009) noted in previous studies of the mouse retina.

The CR6 cells had medium dendritic fields. Because the CR6 cells had very dense and complex dendrites and spines, they seemed to occupy the entire dendritic field area. Their primary dendrites and the many wavy branches of the primary

Fig. 3 The CR1–CR3 types of calretinin-expressing retinotectal retinal ganglion cells in the mouse. (a, b, c) A whole-mount view of an individual cell injected with DiI. (a', b', c') Drawings of each cell. The red color indicates primary dendrites, while the blue color indicates the remaining branches. (a'', b'', c'') The dendritic stratification in the inner plexiform layer of each cell type. CR1 is equivalent to B4 RGCs. CR2 is equivalent to B2 RGCs. CR3 is equivalent to B3 RGCs

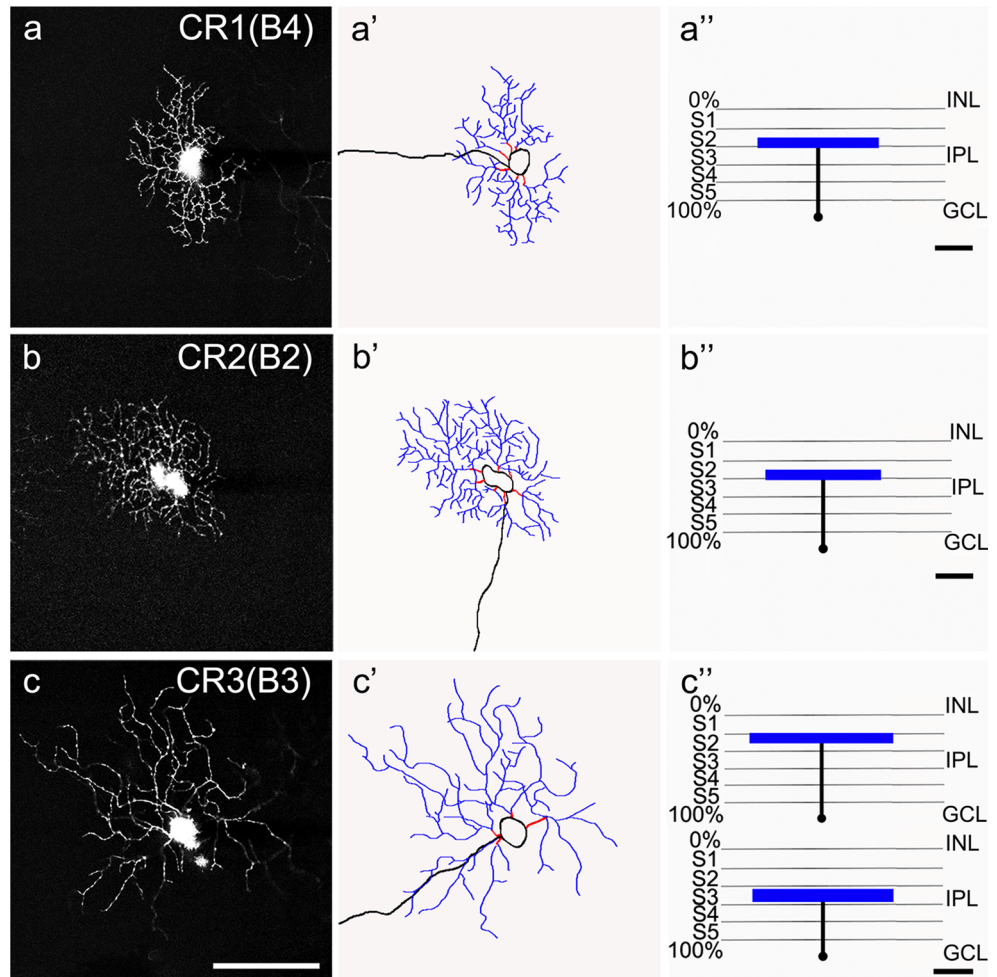
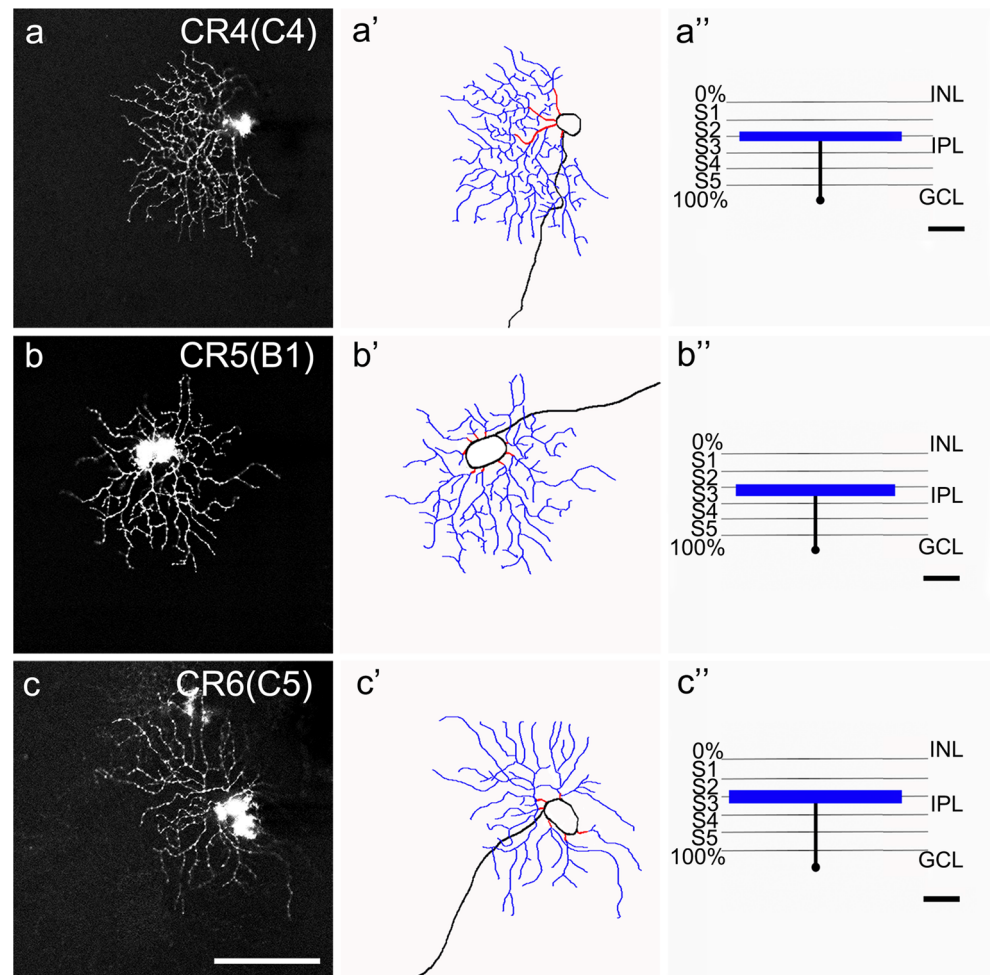


Fig. 4 The CR4–CR6 types of calretinin-expressing retinotectal retinal ganglion cells in the mouse. (a, b, c) A whole-mount view of an individual cell injected with DiI. (a', b') Drawings of each cell. (a'', b'', c'') The dendritic stratification in the inner plexiform layer of each cell type. CR4 is equivalent to C4 RGCs. CR5 is equivalent to B1 RGCs. CR6 is equivalent to C5 RGCs. Scale bar = 100 μ m



dendrites tapered toward the posterior segment border (Fig. 4c, c'). Their dendrites ramified in layer 3 of the IPL (Table 1 and Fig. 4c''). CR6 cells clearly corresponded the C5 cells (Sun et al. 2002), monostratified cluster 1 and 2 cells (Badea and Nathans 2004), cluster 2 cells (Kong et al. 2005), M3 (off) cells (Coombs et al. 2006) and G14 cells (Völgyi et al. 2009) noted in previous studies of the mouse retina.

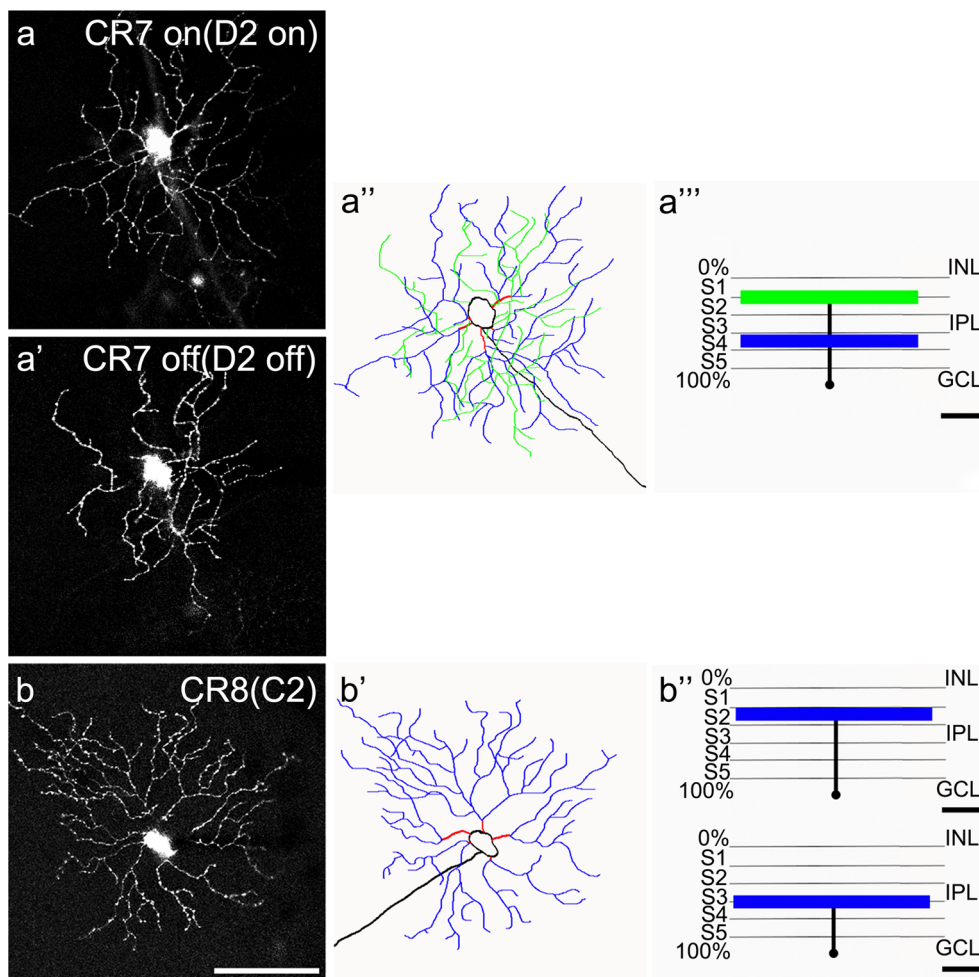
The CR7 cells were analogous to ON-OFF DSGCs with distinct morphological and physiological characteristics (Yang and Masland 1994). The CR7 cells had recursive and loop-forming dendrites (Fig. 5a, a', a''). These cells had a medium dendritic field that arborized in a bistratified manner in both the ON and OFF sublaminae of the IPL (Table 1 and Fig. 5a''). The morphological features of the CR7 cells were similar to the D2 cells (Sun et al. 2002), bistratified cluster 2 and 3 cells (Badea and Nathans 2004), M12/M13/M14 cells (Coombs et al. 2006), G17 cells (Völgyi et al. 2009) and BD cells (Kim et al. 2008) noted in previous studies of the mouse retina.

The CR8 cells had medium-large dendritic fields. The primary and secondary dendrites extended comparatively

straight and they divided into recursive terminal processes that sometimes crossed other branches. These branches extended in disorderly radiating processes (Fig. 5b, b'). The CR8 cells also had ON and OFF varieties. They ramified in the outer part of the IPL (functionally described as the OFF variety) or the inner part of the IPL (functionally described as the ON variety; Table 1 and Fig. 5b''). Inner CR8 cells clearly corresponded to the inner C2 cells (Sun et al. 2002), monostratified cluster 9 cells (Badea and Nathans 2004), cluster 11 cells (Kong et al. 2005), M6 (on) and M10 cells (Coombs et al. 2006), and G10 cells (Völgyi et al. 2009) in the mouse retina. The outer CR8 cells clearly corresponded to outer C2 cells (Sun et al. 2002), monostratified cluster 7 cells (Badea and Nathans 2004), M6 (off) cells (Coombs et al. 2006) and G11 cells (Völgyi et al. 2009) in the mouse retina.

The results of double-labeling retina using antibodies against CR and PV was found in a minority ($9.7 \pm 1.3\%$) of CR-positive cells in the GCL (Fig. 6). In addition, although CR and PV are expressed in various soma-sized cells, CR-positive cells were found mainly in small soma-sized cells, while PV-positive cells were found mainly in large soma-

Fig. 5 The CR7-CR8 types of calretinin-expressing retinotectal retinal ganglion cells in the mouse. (a, a', b) A whole-mount view of an individual cell injected with DiI. (a'', b') Drawings of each cell. (a''', b'') The dendritic stratification in the inner plexiform layer of each cell type. CR7 is equivalent to D2 RGCs. CR7 is equivalent to C2 RGCs. Scale bar = 100 μm



sized cells. Cells expressing both proteins tend to be predominantly small-sized cells but occasionally a few large cells that expressed both markers were also found.

Discussion

The objective of this study was to identify CR-expressing RGCs that projected to the SC in the midbrain. The results

of the present study demonstrated the existence of a subpopulation of CR-expressing retinotectal cells. These cells corresponded with the B1, B2, B3, B4, C2, C4, C5 and D2 cells previously identified by the Sun group (Sun et al. 2002).

Studies are ongoing to determine where the different RGC subtypes project in particular brain regions. For example, a recent study using special transgenic lines and genetic markers to identify each RGC subtype projecting into a special retinal recipient area of the brain has shown that the Pcdh9-

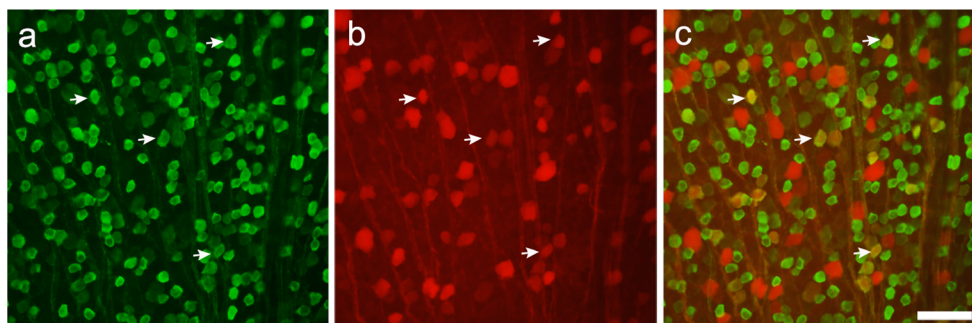


Fig. 6 Micrographs from whole mount of ganglion cell layer labeled with anti-calretinin and anti-parvalbumin antibody. (a) Calretinin-immunoreactive neurons in the ganglion cell layer. (b) Parvalbumin-

immunoreactive neurons in the ganglion cell layer. (c) A few calretinin-immunoreactive cells were double-labeled with parvalbumin (arrows). Scale bar = 50 μm

Cre_{NP276} and Grik4-Cre lines are specific reporter lines for accessory optic nucleus projecting-ON DSGCs (Martersteck et al. 2017). However, most single genes were expressed simultaneously in multiple RGCs. Of course, surprisingly, very few single cells were occasionally defined by a solitary reporter cell line (Huberman et al. 2008, 2009; Kim et al. 2008; Sanes and Masland 2015; Trenholm et al. 2011). It is difficult to find a unique reporter for each cell type and it is unknown how many reporters are necessary to define a type. Therefore, precisely knowing the exact recipient areas of the projections of specific and distinct retinal RGC subtypes labeled by unique reporters is difficult. To avoid these issues, we used a triple-labeling technique that combined retrograde tracer injections in the retinal recipient area and single-cell injections of lipophilic dye after specific protein immunocytochemistry. This advanced technical approach of triple labeling is a way to identify each subtype with the specific molecules in the RGCs that transfer distinct information to specific retinal-recipient areas in the brain.

In our previous study, we analyzed CR-expressing RGCs using single-cell injections in mice. At least ten different cell types expressed CR and these were called A2, B1, B2, B3, B4, C2, C3, C4, C5 and D2 based on the classification by Sun et al. (2002). Compared with those results, the CR-expressing retinotectal RGCs represent a subset of CR-expressing RGCs. The present study describes the morphological heterogeneity of the CR-expressing retinotectal RGCs. These cells exhibit a variety of morphological properties, including monostratified and bistratified dendritic arborizations, branching in the ON and OFF sublaminae of the IPL and sparsely to densely branching dendritic trees. However, of the CR-expressing RGCs, we found that cells with large dendritic fields, such as A2 and C3, did not belong to CR-expressing retinotectal RGCs. CR-expressing retinotectal RGCs in the mouse tended to have small-medium field sizes. The A cells, such as A1 and A2, described by Sun et al. (2002), are the classical alpha RGCs characterized by wide, densely branching dendritic arbors (Boycott and Wässle 1974). Alpha RGCs send information to neurons in a special part of the SC for further processing (Hofbauer and Dräger 1985; Huberman et al. 2008; Kim et al. 2010). In mice, 4 alpha RGC types have been described based on their response to square-wave light stimuli: On-sustained, Off-sustained, ON-transient and Off-transient (Krieger et al. 2017). In particular, quantitative analysis of the colocalization of these cells and calcium-binding proteins revealed that PV was found in a majority of alpha RGCs ($73 \pm 4\%$), calbindin in a minority of alpha RGCs ($27 \pm 2\%$) and CR only in a few alpha RGCs ($13 \pm 4\%$) (Farrow et al. 2013; Münch et al. 2009). Our previous report revealed that alpha retinotectal RGCs contained PV (Yi et al. 2012). In summation, previous and present studies suggest that alpha RGCs in the mouse retina that project to the SC do not contain CR but contain PV instead. These results indicate that protein

heterogeneity may be present in mouse SC-projecting RGCs. In addition, when visual information regarding the transient and sustained light response of alpha RGCs is projected into SC, it may not involve CR.

In mice, studies of RGC classification have been persistently performed after Sun's study (Sun et al. 2002) was performed and studies of their physiological properties and the labeling of their specific subtypes are ongoing. Among the B1, B2, B3, B4, C2, C4, C5 and D2 cells identified by Sun's group (Sun et al. 2002), the B2 and D2 cells are equivalent to the W3 RGCs and ON-OFF DSGCs, respectively (Kim et al. 2010; Sun et al. 2002). However, the other cell types are not well defined. These two cell types mainly respond to motion stimuli. The W3 ganglion cells are the most abundant subtype of the RGCs in mice and the morphological and physiological features of W3 cells are equivalent to local edge detector RGCs and object motion-sensitive RGCs (Kim et al. 2015; Zhang et al. 2012). Combining the previous and present results demonstrates that CR is expressed in W3 cells that project to the SC and that these cells do not express PV (Yi et al. 2012). Thus, the W3 cells that are specialized for detecting the moving stimuli of small objects send this visual information to the SC, which suggests that CR and not PV, might be a molecular participant within W3 cells in the retinotectal pathway.

ON-OFF DSGCs encode directional motion. They mainly project to the SC but some cells project to the LGN, medial terminal nucleus and nucleus of the optic tract (Dhande and Huberman 2014; Kay et al. 2011; Rivlin-Etzion et al. 2011). Combining previous and present results reveals that ON-OFF DSGCs that project to the SC express both CR and PV (Yi et al. 2012). These findings suggest that, in the ON-OFF DSGCs that project to the SC, both CR and PV may help to sustain the structural and physiological bases for directional motion.

Recently, several clusters of orientation-selective RGCs have been defined using calcium imaging in mice and they are present in ON and OFF types (Baden et al. 2016). By comparing their morphological properties, we predicted that OFF orientation-selective cells were reminiscent of the OFF cell types in our data, such as B1 and C5. In addition, the orientation selectivity has been confirmed in the superficial layers of the mouse SC (Wang et al. 2010). Although tracer filling has not yet been performed to determine if they project to the SC, these cells are predicted to contribute to orientation selectivity in the SC through inherited retinotectal projections (Ahmadlou and Heimel 2015; Nath and Schwartz 2016). Thus, only information on morphological similarities is not sufficient to determine this and, thus, further physiological validation is needed. However, we predict that CR-expressing orientation-selective cells project to the SC.

CR was first found in the retina and it has been found in specific neurons of the central and peripheral nervous systems (Schwaller 2014). Because CR can modulate intracellular calcium concentrations, it is considered a calcium-buffering

protein. In addition, CR plays a role as a calcium sensor by interacting with other partners, such as calcium channels. Although the exact function of CR has not been determined, previous studies on CR indicated a putative functional role in neuroprotection. Mice deficient for CR in the cerebellum have motor control impairments (Schiffmann et al. 1999), which could lead to increased neuronal excitability of granule cells (Gall et al. 2003) and alterations in the calcium homeostasis of Purkinje cells (Cheron et al. 2004). We therefore suggest that CR is mainly present in SC-projecting RGCs that respond to motion stimuli, such as W3 and ON-OFF DSGCs. Thus, CR might play a role in neuroprotection by modulating calcium homeostasis or regulating intracellular calcium signaling for the responses to motion stimuli.

In conclusion, we performed experiments involving a new combination of techniques to examine the morphological subtypes of CR-expressing retinotectal RGCs. Among the ten types of CR-positive RGCs described in our previous study, our present results indicated that the eight types of CR-expressing retinotectal RGCs tended to have small-medium fields. However, they were heterogeneous for the morphometric parameters other than their dendritic field size. Although the physiological properties of RGCs have not been completely elucidated, some of these CR-expressing retinotectal RGCs might be morphologically similar to cell types that are related to ON-OFF directional selectivity and local edge detection. Future studies are needed to better understand these mechanisms.

Acknowledgements We thank Cactus Communications for proofreading the manuscript.

Funding This research was supported by the Basic Science Research Program through the National Research Foundation of Korea (NRF), funded by the Ministry of Education (NRF-2016R1D1A1A09918427).

Compliance with ethical standards

Conflict of interest The authors declare that they have no conflict of interest.

Ethical approval All applicable international, national and/or institutional guidelines for the care and use of animals were followed. All procedures involving animals were in accordance with the ethical standards of our institution and were approved by the animal rights committee at Kyungpook National University, Deagu, South Korea (permission NO. 2015-0104). This article does not contain any studies with human participants performed by any of the authors.

Publisher's Note Springer Nature remains neutral with regard to jurisdictional claims in published maps and institutional affiliations.

References

- Ahmadlou M, Heimel JA (2015) Preference for concentric orientations in the mouse superior colliculus. *Nat Commun* 6:6773
- Badea TC, Nathans J (2004) Quantitative analysis of neuronal morphologies in the mouse retina visualized by using a genetically directed reporter. *J Comp Neurol* 480:331–351
- Baden T, Berens P, Franke K, Román Rosón M, Bethge M, Euler T (2016) The functional diversity of retinal ganglion cells in the mouse. *Nature* 529:345–350
- Berson DM (2008) Retinal ganglion cell types and their central projections. In: Basbaum AI, Kaneko A, Shepherd GM, Westheimer G (eds) *The senses: a comprehensive reference*, Vision 1, vol 1. Academic Press, San Diego, pp 491–520
- Boycott BB, Wässle H (1974) The morphological types of ganglion cells of the domestic cat's retina. *J Physiol* 240:397–419
- Callaway EM (2005) Structure and function of parallel pathways in the primate early visual system. *J Physiol* 566:13–19
- Cang J, Feldheim DA (2013) Developmental mechanisms of topographic map formation and alignment. *Annu Rev Neurosci* 36:51–77
- Chen SK, Badea TC, Hattar S (2011) Photoentrainment and pupillary light reflex are mediated by distinct populations of ipRGCs. *Nature* 476:92–95
- Cheron G, Gall D, Servais L, Dan B, Maex R, Schiffmann SN (2004) Inactivation of calcium-binding protein genes induces 160 Hz oscillations in the cerebellar cortex of alert mice. *J Neurosci* 24:434–441
- Coombs J, van der List D, Wang GY, Chalupa LM (2006) Morphological properties of mouse retinal ganglion cells. *Neuroscience* 140:123–136
- Dhande OS, Huberman AD (2014) Retinal ganglion cell maps in the brain: implications for visual processing. *Curr Opin Neurobiol* 24:133–142
- Ecker JL, Dumitrescu ON, Wong KY, Alam NM, Chen SK, LeGates T, Renna JM, Prusky GT, Berson DM, Hattar S (2010) Melanopsin-expressing retinal ganglion-cell photoreceptors: cellular diversity and role in pattern vision. *Neuron* 67:49–60
- Ellis EM, Gauvain G, Sivyer B, Murphy GJ (2016) Shared and distinct retinal input to the mouse superior colliculus and dorsal lateral geniculate nucleus. *J Neurophysiol* 116:602–610
- Farrow K, Masland RH (2011) Physiological clustering of visual channels in the mouse retina. *J Neurophysiol* 105:1516–1530
- Farrow K, Teixeira M, Szikra T, Viney TJ, Balint K, Yonehara K et al (2013) Ambient illumination toggles a neuronal circuit switch in the retina and visual perception at cone threshold. *Neuron* 78:325–338
- Gall D, Roussel C, Susa I, D'Angelo E, Rossi P, Bearzatto B, Galas MC, Blum D, Schurmans S, Schiffmann SN (2003) Altered neuronal excitability in cerebellar granule cells of mice lacking calretinin. *J Neurosci* 23:9320–9327
- Hattar S, Kumar M, Park A, Tong P, Tung J, Yau KW, Berson DM (2006) Central projections of melanopsin-expressing retinal ganglion cells in the mouse. *J Comp Neurol* 497:326–349
- Hattar S, Liao HW, Takao M, Berson DM, Yau KW (2002) Melanopsin-containing retinal ganglion cells: architecture, projections, and intrinsic photosensitivity. *Science* 295:1065–1070
- Haverkamp S, Wässle H (2000) Immunocytochemical analysis of the mouse retina. *J Comp Neurol* 424:1–23
- Hof PR, Young WG, Bloom F (2000) *Comparative cytoarchitectonic atlas of the C57BL/6 and 129/SV: mouse brains*. Elsevier Science, New York
- Hofbauer A, Dräger UC (1985) Depth segregation of retinal ganglion cells projecting to mouse superior colliculus. *J Comp Neurol* 234:465–474
- Huberman AD, Manu M, Koch SM, Susman MW, Lutz AB, Ullian EM, Baccus SA, Barres BA (2008) Architectures and activity-mediated refinement of axonal projections from a mosaic of genetically identified retinal ganglion cells. *Neuron* 59:425–438
- Huberman AD, Wei W, Elstrott J, Stafford BK, Feller MB, Barres BA (2009) Genetic identification of an on-off direction-selective retinal ganglion cell subtype reveals layer-specific subcortical map of posterior motion. *Neuron* 62:327–334

- Ito S, Feldheim DA (2018) The mouse superior colliculus: an emerging model for studying circuit formation and function. *Front Neural Circuits* 12:10
- Jeon CJ, Strettoi E, Masland RH (1998) The major cell populations of the mouse retina. *J Neurosci* 18:8936–8946
- Jonathan W, Hiroshi H (2017) Visual system architecture. In: Pablo A (ed) *Handbook of visual optics, volume one: fundamentals and eye optics*. Fundamentals. CRC Press, Boca Raton, pp 159–180
- Kao YH, Sterling P (2003) Matching neural morphology to molecular expression: single cell injection following immunostaining. *J Neurocytol* 32:245–251
- Kay JN, De la Huerta I, Kim IJ, Zhnag Y, Yamagata M, Chu MW, Meister M, Sanes JR (2011) Retinal ganglion cells with distinct directional preferences differ in molecular identity, structure, and central projections. *J Neurosci* 31:7753–7762
- Kim IJ, Zhang Y, Meister M, Sanes JR (2010) Laminar restriction of retinal ganglion cell dendrites and axons: subtype-specific developmental patterns revealed by transgenic markers. *J Neurosci* 30:1452–1462
- Kim IJ, Zhang Y, Yamagata M, Meister M, Sanes JR (2008) Molecular identification of a retinal cell type that responds to upward motion. *Nature* 452:478–482
- Kim T, Soto F, Kerschensteiner D (2015) An excitatory amacrine cell detects object motion and provides feature-selective input to ganglion cells in the mouse retina. *elife*. <https://doi.org/10.7554/eLife.08025>
- Kim TJ, Jeon CJ (2006) Morphological classification of parvalbumin-containing retinal ganglion cells in mouse: single-cell injection after immunocytochemistry. *Invest Ophthalmol Vis Sci* 47:2757–2764
- Kong JH, Fish DR, Rockhill RL, Masland RH (2005) Diversity of ganglion cells in the mouse retina: unsupervised morphological classification and its limits. *J Comp Neurol* 489:293–310
- Krieger B, Qiao M, Rousso DL, Sanes JR, Meister M (2017) Four alpha ganglion cell types in mouse retina: function, structure, and molecular signatures. *PLoS One* 12(7):e0180091
- Kwon OJ, Lee ES, Jeon CJ (2014) Density and types of calretinin-containing retinal ganglion cells in rabbit. *Neuroscience* 278:343–353
- Lee ES, Lee JY, Jeon CJ (2010) Types and density of calretinin-containing retinal ganglion cells in mouse. *Neurosci Res* 66:141–150
- Martersteck EM, Hirokawa KE, Evarnts M, Bernard A, Duan X, Li Y, Ng L, Oh SW, Ouellette B, Royall JJ, Stoecklin M, Wang Q, Zeng H, Sanes JR, Harris JA (2017) Diverse central projection patterns of retinal ganglion cells. *Cell Rep* 18:2058–2072
- May PJ (2006) The mammalian superior colliculus: laminar structure and connections. *Prog Brain Res* 151:321–378
- Münch TA, da Silveira RA, Siebert S, Viney TJ, Awatramani GB, Roska B (2009) Approach sensitivity in the retina processed by a multifunctional neural circuit. *Nat Neurosci* 12:1308–1316
- Nath A, Schwartz GW (2016) Cardinal orientation selectivity is represented by two distinct ganglion cell types in mouse retina. *J Neurosci* 36:3208–3221
- Rivlin-Etzion M, Zhou K, Wei W, Elstrott J, Nguyen PL, Barres BA, Huberman AD, Feller MG (2011) Transgenic mice reveal unexpected diversity of on-off direction-selective retinal ganglion cell subtypes and brain structures in motion processing. *J Neurosci* 31:8760–8769
- Rockhill RL, Euler T, Masland RH (2000) Spatial order within but not between types of retinal neurons. *Proc Natl Acad Sci U S A* 97:2303–2307
- Rodieck RW (1998) *The first steps in seeing*. Sinauer Associates, Sunderland
- Roska B, Meister M (2014) The retina dissects the visual scene in distinct features. In: Werner JS, Chalupa LM (eds) *The new visual neuroscience, retinal mechanisms and processes*. MIT Press, Cambridge, pp 163–182
- Sanes JR, Masland RH (2015) The types of retinal ganglion cells: current status and implications for neuronal classification. *Annu Rev Neurosci* 38:221–246
- Schiffmann SN, Cheron G, Lohof A, d'Alcantara P, Meyer M, Parmentier M, Schurmans S (1999) Impaired motor coordination and Purkinje cell excitability in mice lacking calretinin. *Proc Natl Acad Sci U S A* 96:5257–5262
- Schmolesky M (1995–2005) The primary visual cortex. In: Kolb H, Fernandez E, Nelson R (eds) *Webvision, The Organization of the Retina and Visual System* (Internet). University of Utah Health Sciences Center, Salt Lake City
- Schwaller B (2014) Calretinin: from a “simple” Ca(2+) buffer to a multifunctional protein implicated in many biological processes. *Front Neuroanat*. eCollection 2014. <https://doi.org/10.3389/fnana.2014.00003>
- Stein BE, Wallace MW, Stanford TR, Jiang W (2002) Cortex governs multisensory integration in the midbrain. *Neuroscientist* 8:306–314
- Sun W, Li N, He S (2002) Large-scale morphological survey of rat retinal ganglion cells. *Vis Neurosci* 19:483–493
- Trenholm S, Johnson K, Li X, Smith RG, Awatramani GB (2011) Parallel mechanisms encode direction in the retina. *Neuron* 71:683–694
- Völgyi B, Chheda S, Bloomfield SA (2009) Tracer coupling patterns of the ganglion cell subtypes in the mouse retina. *J Comp Neurol* 512:664–687
- Wang L, Sarnaik R, Rangarajan K, Liu X, Cang J (2010) Visual receptive field properties of neurons in the superficial superior colliculus of the mouse. *J Neurosci* 30:16573–16584
- Yang G, Masland RH (1994) Receptive fields and dendritic structure of directionally selective retinal ganglion cells. *J Neurosci* 14:5267–5280
- Yi CW, Yu SH, Lee ES, Lee JG, Jeon CJ (2012) Types of parvalbumin-containing retinotectal ganglion cells in mouse. *Acta Histochem Cytochem* 45:201–210
- Zhang Y, Kim IJ, Sanes JR, Meister M (2012) The most numerous ganglion cell type of the mouse retina is a selective feature detector. *Proc Natl Acad Sci U S A* 109:E2391–E2398